Plant Cell Reports (2023) 42:1791–1808
https://doi.org/10.1007/s00299-023-03066-x

ORIGINAL ARTICLE

Molecular characterization of *oleosin* genes in *Cyperus esculentus*, a Cyperaceae plant producing oil in underground tubers

Zhi Zou[1] · Yujiao Zheng[1] · Zhongtian Zhang[1] · Yanhua Xiao[1] · Zhengnan Xie[1] · Lili Chang[1] · Li Zhang[1,2] · Yongguo Zhao[1,3]

Received: 28 June 2023 / Accepted: 25 August 2023 / Published online: 25 September 2023

Abstract

Key message ***CeOLE*** **genes exhibit a tuber-predominant expression pattern and their mRNA/protein abundances are positively correlated with oil accumulation during tuber development. Overexpression could significantly increase the oil content of tobacco leaves.**

Abstract Oleosins (OLEs) are abundant structural proteins of lipid droplets (LDs) that function in LD formation and stabilization in seeds of oil crops. However, little information is available on their roles in vegetative tissues. In this study, we present the first genome-wide characterization of the *oleosin* family in tigernut (*Cyperus esculentus* L., Cyperaceae), a rare example accumulating high amounts of oil in underground tubers. Six members identified represent three previously defined clades (i.e. U, SL and SH) or six out of seven orthogroups (i.e. U, SL1, SL2, and SH1–3) proposed in this study. Comparative genomics analysis reveals that lineage-specific expansion of Clades SL and SH was contributed by whole-genome duplication and dispersed duplication, respectively. Moreover, presence of SL2 and SH3 in *Juncus effuses* implies their appearance sometime before Cyperaceae-Juncaceae divergence, whereas SH2 appears to be Cyperaceae specific. Expression analysis showed that *CeOLE* genes exhibit a tuber-predominant expression pattern and transcript levels are considerably more abundant than homologs in the close relative *Cyperus rotundus*. Moreover, *CeOLE* mRNA and protein abundances were shown to positively correlate with oil accumulation during tuber development. Additionally, two dominant isoforms (i.e. CeOLE2 and -5) were shown to locate in LDs as well as the endoplasmic reticulum of tobacco (*Nicotiana benthamiana*) leaves, and are more likely to function in homo and heteromultimers. Furthermore, overexpression of *CeOLE2* and *-5* in tobacco leaves could significantly increase the oil content, supporting their roles in oil accumulation. These findings provide insights into lineage-specific family evolution and putative roles of *CeOLE* genes in oil accumulation of vegetative tissues, which facilitate further genetic improvement for tigernut.

Keywords Oil crop · Oil accumulation · Expression divergence · Orthogroup · Protein interaction · Synteny analysis

Introduction

In the seed of oil crops, triacylglycerols (TAGs) stored in lipid droplets (LDs) represent the major energy and carbon reserve for seed germination and subsequent seedling growth (Huang 2018; Guzha et al. 2023). LDs are enclosed by a layer of phospholipids and several structural proteins (Hsieh and Huang 2004). Among these proteins, oleosins (OLEs) are most abundant and feature a long central hydrophobic hairpin of approximately 72 residues ($X_{30}PX_5SPX_3PX_{30}$), which penetrates the TAG core and functions to stabilize the LD (Abell et al. 1997; Shimada et al. 2008; Brocard et al. 2017). On the contrary, sequences at the N- and C-terminals, which lie on the phospholipid surface, are usually amphipathic and variable (Huang 2018). Generally, oleosins possess a small molecular weight of 14–30 kilodalton (kDa) (Huang and Huang 2015; Zou et al. 2022a). Since their first appearance in green algae, the *oleosin* family has highly expanded and diverged in terrestrial plants and 2–53 members representing five clades, i.e., U (universal), SL (seed low-molecular-weight), SH (seed high-molecular-weight), T (tapetum in Brassicaceae), and M (mesocarp in Lauraceae), have been described (Schein et al. 2004; Huang and Huang 2015;

Communicated by Wei Ma.

Zhi Zou, Yujiao Zheng and Zhongtian Zhang contributed equally.

Extended author information available on the last page of the article

Jia et al. 2022; Zou et al. 2022a). Interestingly, accumulation of oleosins in seeds not only determines the LD size but also positively relates to the oil content (Siloto et al. 2006; Zhang et al. 2019). Nevertheless, despite their high abundance in seeds as well as pollen and tapetum cells, oleosins have rarely been found in the LDs of fruits and leaves (Hsieh and Huang 2004; Horn et al. 2013; Kretzschmar et al. 2020).

Cyperus esculentus L., commonly known as yellow nutsedge or tigernut, is an herbaceous perennial C_4 plant of the Cyperaceae (sedge) family within Poales (De Castro et al. 2015; Xiao et al. 2022; Zou et al. 2021, 2023a, b). Unlike most Poaceae species predominately accumulating starch in their seeds, tigernut is the only known species that produces high amounts of oil (up to 35%) in underground tubers, which is also different from its close relative purple nutsedge (*Cyperus rotundus*, Cyperaceae) as well as oil palm (*Elaeis guineensis*), an Arecaceae plant bearing oil in the fruit mesocarp instead (Stoller and Weber 1975; Turesson et al. 2010; Singh et al. 2013; Codina-Torrella et al. 2015; Zou et al. 2021; Xu et al. 2022). Oil extracted from tigernut tubers, which is mainly composed of oleic acid (up to 80%), can be consumed as healthy edible oil or as an alternative resource of biodiesel fuel (Zhang et al. 1996; Barminas et al. 2001; Makareviciene et al. 2013; Maduka and Ire 2018). Tigernut is a promising oil crop for its high yield and wide regional adaptability, including tropical, subtropical, temperate as well as cold zones (Stoller and Sweet 1987; De Castro et al. 2015; Zou et al. 2022b). It has been reported that tigernut can produce 4.5–12 t tubers per hectare, which means that its oil yield could reach up to approximately 90–240 kg per acre, lower than oil palm but much higher than most oilseed crops such as maize (*Zea mays*), rapeseed (*Brassica napus*), and soybean (*Glycine max*) (Makareviciene et al. 2013; Maduka and Ire 2018). Compared with oilseed crops, the mechanism of oil accumulation in tigernut tubers is poorly understood.

According to our previous study, rapid accumulation of oil during tuber development is accompanied by the increasing numbers of LDs (Jin et al. 2010). More recently, proteome analysis of LD-enriched fractions of tigernut tubers revealed the high abundance of oleosins (Niemeyer et al. 2022). Given essential roles of oleosins in LD formation and stabilization (Siloto et al. 2006; Shimada et al. 2008; Zhang et al. 2019; Ojha et al. 2021), in this study, we conducted a genome-wide characterization of the *oleosin* family in tigernut, including gene localizations, gene structures, sequence characteristics, and evolutionary patterns. Moreover, correlation of *CeOLE* mRNA/protein abundance with oil accumulation during tuber development, subcellular localizations, protein interaction patterns, and overexpressing in tobacco (*Nicotiana benthamiana*) were also investigated, which provide valuable information for further functional analysis and genetic improvement in this special species.

Materials and methods

Plant materials

In this experiment, a tigernut variety named Reyan3 (Zou et al. 2021) was used, which was cultivated in sandy soil in the Wenchang city of Hainan province, China. At approximately 7 days after sowing (DAS), shoots started to emerge above soil from seed tubers. At about 30 DAS, new tubers started to develop at the apex of stolons. To determine the dry mass and oil content, tubers were periodically collected from the onset of tuber initiation until maturation, spanning about 35 d as described before (Zou et al. 2022b). Since tubers appear throughout the growth cycle, this study adopted the term DAI (days after tuber initiation) instead of DAS used by several researchers (Jin et al. 2010; Bai et al. 2021; Wang et al. 2021). For gene cloning, gene expression analysis, and protein quantification, fresh tubers of representative stages (i.e. 1, 3, 5, 10, 15, 20, 25, and 35 DAI) were quickly freezed with liquid nitrogen and stored at −80 °C. Additionally, young leaves were also collected for genomic DNA extraction. For analyses of bimolecular fluorescence complementation (BiFC), subcellular localization, and oil regulation, tobacco were grown as previously described (Qiao et al. 2022a; Xu et al. 2022).

Identification of *oleosin* family genes by using public datasets

As shown in Supplementary Table S1, *oleosin* genes described in rice (*Oryza sativa*), arabidopsis (*Arabidopsis thaliana*), and *Amborella trichopoda* (Huang and Huang 2015; Zou et al. 2022a) were obtained from RGAP7 (http://rice.plantbiology.msu.edu/), TAIR11 (https://www.arabidopsis.org/), and Phytozome v13 (https://phytozome.jgi.doe.gov/pz/portal.html), respectively. Genomic and transcriptome data of tigernut, purple nutsedge, *Carex littledalei*, *C. myosuroides*, *Rhynchospora breviuscula*, and *Juncus effusus* were accessed from CNGBdb (https://db.cngb.org/search/assembly/CNA0051961/) and NCBI (https://www.ncbi.nlm.nih.gov/). RNA sequencing (RNA-seq) reads (NCBI Project accession no. PRJNA671562, 150 bp paired-ends) of purple nutsedge tubers were de novo assembled using Trinity (v2.13.2, https://github.com/trinityrnaseq/trinityrnaseq/wiki), which resulted in 31,192 unigenes for the construction of an in-house library. To identify *oleosin* family genes, HMMER (v3.3, http://hmmer.janelia.org/) searches were performed using the Pfam profile PF01277 (v35.0, https://pfam.xfam.org/). Gene models of candidates were further curated with

mRNAs when available, and presence of the conserved oleosin domain in deduced proteins was confirmed by Pfam Search.

Sequence alignment and phylogenetic analysis

Nucleotide and protein multiple sequence alignments were conducted using ClustalW and MUSCLE implemented in MEGA6 (Tamura et al. 2013), respectively. The result of protein sequence alignment was displayed using Boxshade (https://embnet.vital-it.ch/software/BOX_form.html), and phylogenetic tree construction was performed using MEGA6 with the maximum likelihood method and bootstrap of 1000 replicates. Systematic names of *oleosin* family genes were assigned with two italic letters denoting the source organism and a progressive number based on sequence similarity. To distinguish them from the *oleosin* genes in arabidopsis, three italic letters were used in *A. trichopoda* (i.e. *AtrOLE1–5*).

Synteny analysis, definition of orthogroups (OGs), and calculation of evolutionary rate

Synteny analysis was carried out as previously described (Zou et al. 2019), where duplicate pairs were identified using the all-to-all BLASTp method and syntenic blocks were inferred using MCScanX (*E*-value, 1e-10; BLAST hits, 5) (Wang et al. 2012). Different modes of gene duplication were identified using the DupGen_finder pipeline (Qiao et al. 2019), and Ks (synonymous substitution rate) and Ka (nonsynonymous substitution rate) of duplicate pairs were calculated using TBtools (Chen et al. 2020). Orthologs between different species were identified using the best-reciprocal-hit (BRH) method, and orthogroups were assigned only when they are present in at least two species examined.

Protein properties and conserved motif analysis

Physiochemical parameters such as theoretical molecular weight (MW), isoelectric point (pI), aliphatic index (AI), and grand average of hydropathicity (GRAVY) of oleosins were calculated using ProtParam (http://web.expasy.org/protparam/). Transmembrane helices (TMHs) and Kyte–Doolittle hydrophobicity plots were predicted using TMHMM (v2.0, https://services.healthtech.dtu.dk/service.php?TMHMM-2.0) and ProtScale (https://web.expasy.org/protscale/), respectively. Conserved motifs were identified using MEME (v5.4.1, https://meme-suite.org/tools/meme) with optimized parameters of any number of repetitions, maximum number of 15 motifs, and the width of 6 and 120 residues for each motif.

Genomic DNA extraction and gene cloning

Genomic DNA extraction was conducted using a modified CTAB method as previously described (Zhao and Wei 2011). Primers used for gene isolation are shown in Supplementary Table S2, whereas PCR amplification was performed with the following reaction conditions: pre-denaturation at 95 °C for 3 min, denaturation for 35 cycles at 95 °C for 30 s, annealing at 60 °C for 30 s, and extension at 72 °C for 40 s, and a final extension at 72 °C for 5 min. PCR products were cloned into the *p*MD-18 T vector (TaKaRa Bio Inc., Dalian) for subsequent Sanger sequencing.

Gene expression analysis based on RNA-seq

Global expression profiles of *oleosin* genes in tigernut and yellow nutsedge were investigated using transcriptome datasets as shown in Supplementary Table S3. Raw sequence reads in the FASTQ format were obtained using fastq-dump, and quality control was performed using fastQC (https://www.bioinformatics.babraham.ac.uk/projects/fastqc/). Read mapping was performed using Bowtie 2 (Langmead and Salzberg 2012), and relative expression level of each transcript was presented as FKPM (fragments per kilobase of exon per million fragments mapped) (Mortazavi et al. 2008). Expression profile data of *oleosin* genes in rice was accessed from BAR (http://bar.utoronto.ca/).

Gene expression analysis based on qRT-PCR

Total RNA extraction, synthesis of the first-strand cDNA, and qRT-PCR analysis were performed as described before (Zou et al. 2022b). All qRT-PCR assays were conducted in triplicate for each biological sample with two reference genes *CeTUB4* and *CeUCE2* as reported before (Bai et al. 2021). Relative gene abundance was estimated with the $2^{-\Delta\Delta Ct}$ method and statistical analysis was performed using SPSS Statistics 20 as previously described (Zou et al. 2015).

4D-parallel reaction monitoring (4D-PRM)-based protein quantification

Proteomic data of tigernut and purple nutsedge, which was accessed from ProteomeXchange/PRIDE (PXD021894, PXD031123, and PXD035931), was analyzed using Maxquant (v1.6.15.0) as previously described (Wang et al. 2020). Based on their abundance, two dominant isoforms, i.e., CeOLE2 and -5, were selected for 4D-PRM analysis, and related unique peptides are shown in Supplementary

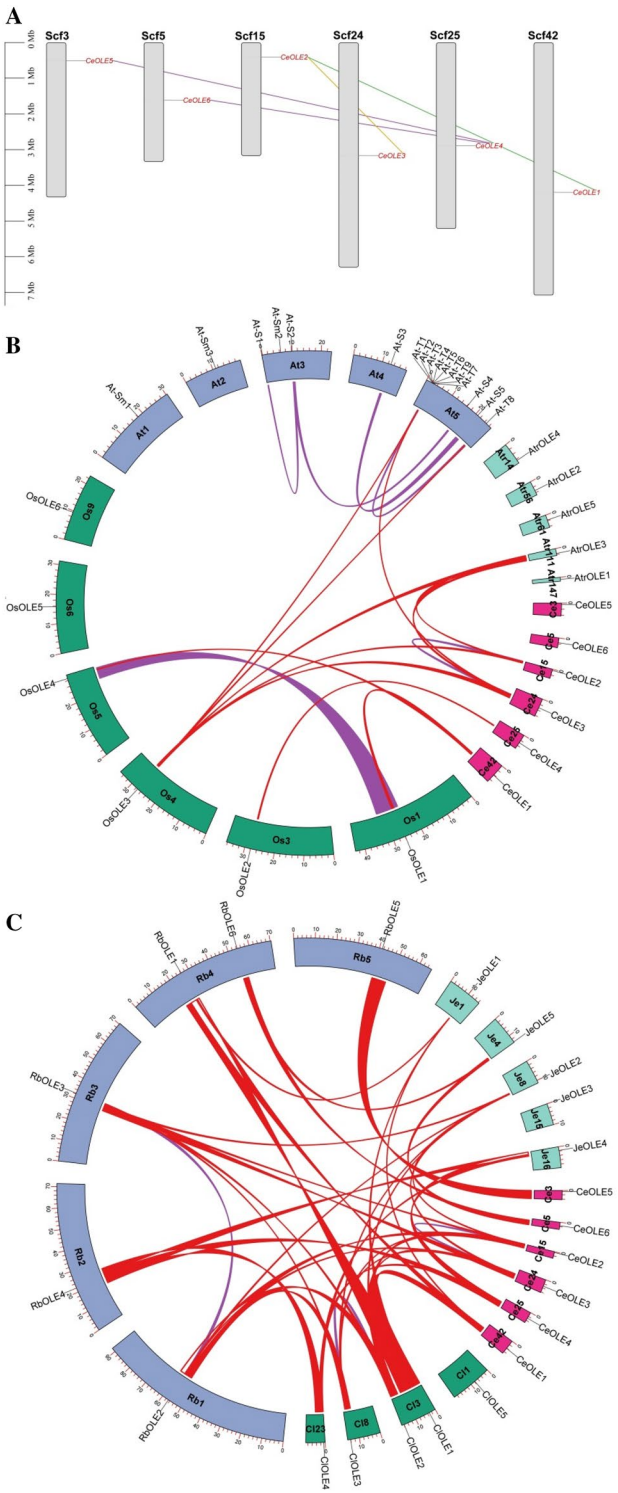

Fig. 1 Duplication events of *CeOLE* genes and synteny analysis within and between tigernut and representative species. **A** Duplication events detected in tigernut. Serial numbers are indicated at the top of each scaffold, and the scale is in Mb. Duplicate pairs identified in this study are connected using lines in different colors, i.e., transposed (green), dispersed (purple), and WGD (gold). **B** Synteny analysis within and between tigernut, rice, arabidopsis, and *A. trichopoda*. **C** Synteny analysis within and between tigernut, *C. littledalei*, *R. breviuscula*, and *J. effusus*. Shown are *oleosin*-encoding chromosomes/scaffolds and only syntenic blocks that contain *oleosin* genes are marked. (At, *A. thaliana*; Atr, *A. trichopoda*; Ce, *C. esculentus*; Chr, chromosome; Cl, *C. littledalei*; Je, *J. effusus*; Mb, megabase; OLE, oleosin; Rb, *R. breviuscula*; Os, *O. sativa*; Scf, scaffold; WGD, whole-genome duplication) (color figure online)

Table S4. Protein extraction, trypsin digestion, and LC–MS/MS analysis were conducted as described before (Wang et al. 2020).

BiFC, subcellular localization, and functional analysis on oil accumulation

Plasmid construction and *Agrobacterium tumefaciens*-mediated transformation were carried out as previously described (Qiao et al. 2022a; Xu et al. 2022), where primers used are shown in Supplementary Table S2. Briefly, the coding sequence (CDS) without the termination codon was cloned into *p*NC-BiFC-Ecn, *p*NC-BiFC-Enn, *p*NC-Cam1304-SubC, and *p*CAMBIA1301 by Nimble Cloning (Yan et al. 2023), and resulted recombinant plasmids were introduced into GV3101 with the helper plasmid *p*Soup-*P19*. *Agrobacterium* solution with an OD_{600} of 0.8 was collected and suspended using the infiltrating solution that includes 10 mmol/L $MgCl_2$, 10 mmol/L MES, and 150 µmol/L acetosyringone (pH = 5.6). Tobacco leaves of approximately 4-week-old plants were infiltrated, which were later processed for confocal laser scanning microscopy imaging (Zeiss LMS880, Germany). All assays were performed across three different leaves at the same position of independent plants. For subcellular localization analysis, the endoplasmic reticulum (ER) marker RFP-HDEL (Gong et al. 2021) was employed. The wavelength of laser-1 was set as 610 nm for RFP observation, where the fluorescence was excited at 587 nm and detected at a band width of 565–700 nm. The wavelength of laser-2 was set as 517 nm for EGFP observation, where the fluorescence was excited at 493 nm and detected at a band width of 400–580 nm. The wavelength of laser-3 was set as 470 nm for chlorophyll autofluorescence observation, where the fluorescence was excited at 633 nm and detected at a band width of 650–690 nm. For oil regulation, transformed leaves were collected at one, three, and five days after infiltration, which were subject to qRT-PCR analysis and TAG determination as described before (Jin et al. 2010; Xu et al. 2022).

Results

Identification, gene localization, and synteny analysis of *oleosin* genes in tigernut

As shown in Fig. 1A and Supplementary Table S1, mining the tigernut genome resulted in six *oleosin* genes from

six scaffolds (Scf). The family numbers are equal to that present in rice, one more than five reported in *A. trichopoda*, and considerably less than 17 described in arabidopsis (Supplementary Table S1). The CDS length of *CeOLE* genes varies from 423 to 483 base pairs (bp), putatively encoding 140–160 amino acids (AA) with the MW of 14.33–16.25 kDa; the theoretical pI values are all above 7 (9.46–10.19), indicating their alkaline characteristic. As expected, all of them possess similar Kyte–Doolittle hydrophobicity plots (Supplementary Fig. S1), and exhibit the amphipathic property with high AI values (94.57–106.90) and GRAVY values of more than 0 (0.344–0.577) (Supplementary Table S1). Besides harboring one 113-AA oleosin domain that includes the highly conserved proline knot motif (PX_5SPX_3P) (Fig. 2A), CeOLE proteins were shown to contain two to three TMHs (Supplementary Table S1).

Protein sequence similarities within the *CeOLE* gene family vary from 37.0% to 72.5%, and relatively high similarities were observed between two pairs, i.e., 68.5% and 72.5% for CeOLE2/-3 and CeOLE4/-5, respectively (Supplementary Table S5), implying their recent origin. Indeed, intraspecies synteny analysis showed that *CeOLE2* and *-3* are located within syntenic blocks of tigernut scaffolds (Fig. 1B). Moreover, interspecies synteny analysis revealed that both *CeOLE2* and *-3* are syntelogs of *OsOLE3* and *AtrOLE3*, though only *CeOLE3* was identified as the syntelog of *At-T5* (Fig. 1B), implying their appearance sometime after tigernut-rice divergence. As for *CeOLE4* and *-5* that are not located within syntenic blocks, only *CeOLE4* was characterized as the syntelog of *OsOLE2* (Fig. 1B), thereby, they were defined as dispersed repeats. Additionally, *CeOLE6* was also defined as a dispersed repeat of *CeOLE4*, whereas *CeOLE1* and *-2* were characterized as transposed repeats, which is consistent with *OsOLE3* that was identified as the transposed repeat of *OsOLE4* (Supplementary Table S1).

Characterization of *oleosin* genes in representative species and insight into lineage-specific family evolution in Cyperaceae

Since the origin of *CeOLE5* and *-6* was not well resolved by synteny analysis as described above, we thereby took advantage of available genome and transcriptome data to identify homologs from representative species of the Cyperaceae family (i.e. purple nutsedge, *C. littledalei*, *C. myosuroides*, and *R. breviuscula*) as well as its close family Juncaceae (i.e. *J. effuses*) (Can et al. 2020; Hofstatter et al. 2022; Ning et al. 2023). As a result, five to six *oleosin* family genes were identified, which were shown to distribute across four to five chromosomes (Chr). It is worth noting that, in contrast to *RbOLE1* and *-6* that are co-located on Chr4, *ClOLE1* and *CmOLE1* are, respectively, co-located with *ClOLE2* and *CmOLE2* on Chr3 (Supplementary Table S1), implying species or genus-specific chromosomal rearrangement.

To uncover their evolutionary relationships, an unrooted phylogenetic tree was constructed using full-length oleosins present in tigernut, purple nutsedge, *C. littledalei*, *C. myosuroides*, *R. breviuscula*, *J. effusus*, rice, arabidopsis, and *A. trichopoda*. As shown in Fig. 2B, these oleosins were grouped into four clades, i.e., U, SL, SH, and T, where T is arabidopsi-specific. Obviously, Clades SL and SH in Cyperaceae could be further divided into two and three groups that were denoted as SL1, SL2, and SH1–3, respectively, which is consistent with BRH-based homologous analysis as shown in Table 1. Two main differences are that AtrOLE4 was assigned into SH1, whereas AtrOLE5 and OsOLE5 were shown to form one additional OG named SH4 (Table 1). Despite frequent occurrence of chromosome fission and fusion in Cyperaceae species (Can et al. 2020; Hofstatter et al. 2022; Ning et al. 2023; Zhao et al. 2023), a high level of collinearity relation was observed between *oleosin*-encoding regions, though SH3 is absent from *C. littledalei* for gene fragmentation (one gene fragment was identified on Chr11) and *ClOLE5* is no longer located within syntenic blocks (Fig. 1C). Moreover, presence of SL2 (i.e. *JeOLE3*) and SH3 (i.e. *JeOLE5*) homologs in *J. effusus* but not rice (Table 1) implies their appearance sometime before Cyperaceae-Juncaceae divergence but after Cyperaceae-Poaceae split. Interestingly, as observed in tigernut, SL1 and -2 homologs are also located within syntenic blocks of *C. littledalei* and *R. breviuscula* (Fig. 1C), suggesting that they may be generated by one whole-genome duplication (WGD) event shared by Cyperaceae and Juncaceae after the split with Poaceae. Although a relatively high similarity of 75.3% was observed between JeOLE2 and -3 (Supplementary Table S5), possible transposition or chromosome rearrangement may occur in the *JeOLE3*-encoding region in contrast to the conserved evolution of that of *JeOLE2* (Fig. 1C). The absence of a SH2 homolog in *J. effusus* as well as rice indicates that this group is more likely to be Cyperaceae-specific, generated via an unknown mechanism sometime after Cyperaceae-Juncaceae divergence, which is consistent with relatively higher sequence similarities (63.9–71.1% vs 71.9–75.5%) and smaller Ks values (5.2337–10.5926 vs 8.4319–51.8549) between SH1 and -2 than that between SL1 and -2 (Table 2). Moreover, variable Ks values also imply different evolutionary rate between these species. Nevertheless, low Ka/Ks ratios from 0.0045 to 0.2750 (Table 2) indicate that paralogs were stabilized mainly by purifying selection.

Although most *CeOLE* genes were shown to be intronless, *CeOLE5* possesses one intron immediately after the sequence encoding the hydrophobic hairpin stretch (Fig. 3B), which is confirmed by gene cloning using tigernut genomic DNA as template. Interestingly, the intron was shown to be highly conserved in SH2 homologs of Cyperaceae species, varying from

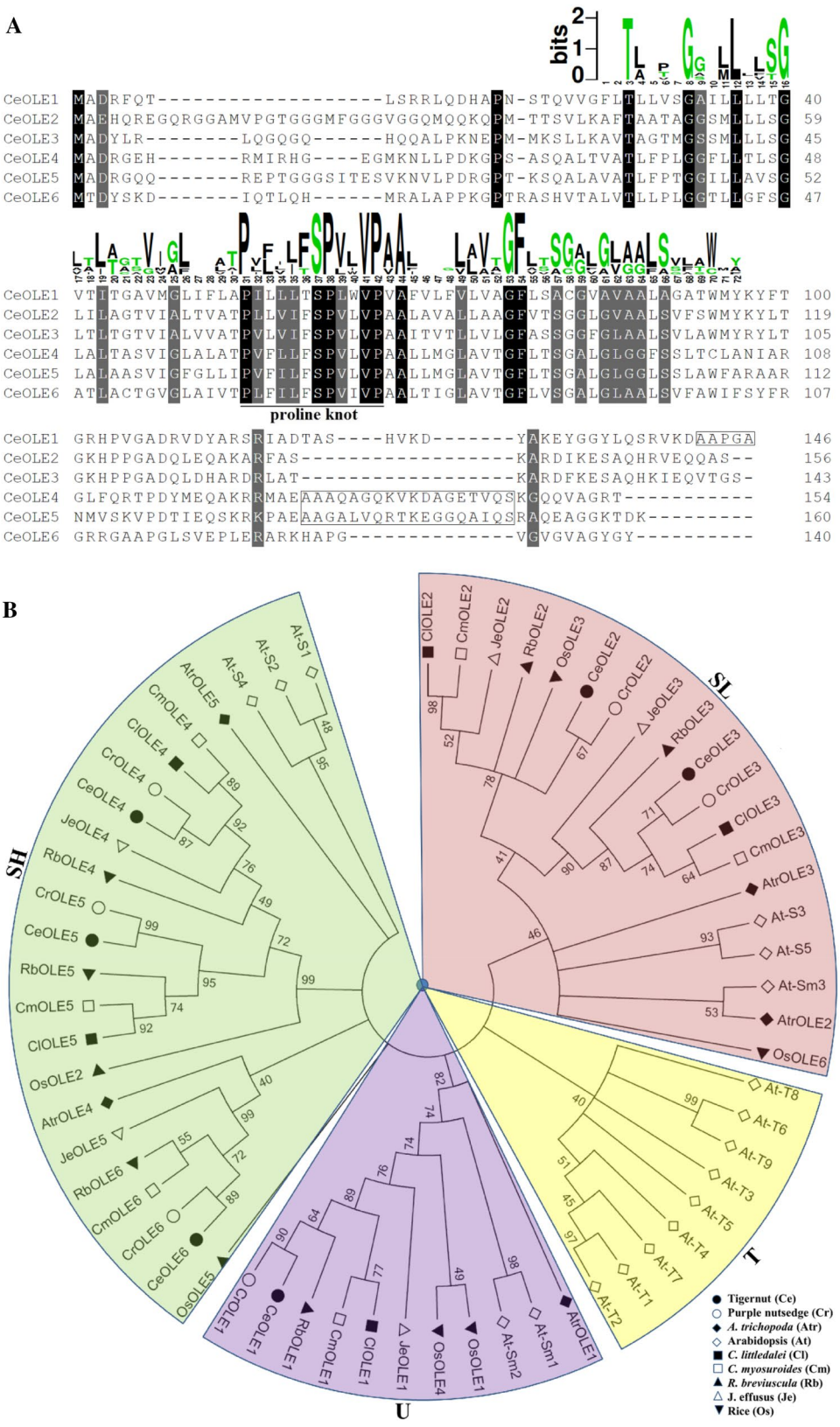

Fig. 2 Multiple sequence alignment and phylogenetic analysis of oleosins. **A** Sequence alignment and structural features of six CeOLE proteins. Sequence alignment and display were conducted using MUSCLE and Boxshade, respectively. Identical and similar amino acids are highlighted in black or dark grey, respectively. The SeqLogo of the 72-residue proline knot motif is shown above the alignment, and the PX_5SPX_3P pattern is underlined. The C-terminal AAPGA of Clade U and the putative C-terminal insertion of Clade SH are boxed. **B** Phylogenetic analysis of CeOLEs with homologs from other species. Shown is an unrooted phylogenetic tree resulting from full-length oleosins with MEGA6 (maximum likelihood method and bootstrap of 1,000 replicates), where the distance scale denotes the number of amino acid substitutions per site and the name of each clade is indicated next to the corresponding group. (At, *A. thaliana*; Atr, *A. trichopoda*; Ce, *C. esculentus*; Cl, *C. littledalei*; Cm, *C. myosuroides*; *C. rotundus*; Je, *J. effusus*; OLE, oleosin; Rb, *R. breviuscula*; Os, *O. sativa*; SH, seed high-molecular-weight; SL, seed low-molecular-weight; T, tapetum; U, universal)

Table 1 Seven orthogroups identified on the basis of analyzing nine representative species

Clade	OG	Tigernut	Purple nutsedge	*C. littledalei*	*C. myosuroides*	*R. breviuscula*	*J. effusus*	Rice	Arabidopsis	*A. trichopoda*
U	U1	CeOLE1	CrOLE1	ClOLE1	CmOLE1	RbOLE1	JeOLE1	OsOLE4 OsOLE1	At-Sm1 At-Sm2	AtrOLE1
SL	SL1	CeOLE2	CrOLE2	ClOLE2	CmOLE2	RbOLE2	JeOLE2	OsOLE3 OsOLE6	At-S3 At-S5 At-Sm3	AtrOLE2 AtrOLE3
	SL2	CeOLE3	CrOLE3	ClOLE3	CmOLE3	RbOLE3	JeOLE3	ND	ND	ND
SH	SH1	CeOLE4	CrOLE4	ClOLE4	CmOLE4	RbOLE4	JeOLE4	OsOLE2	At-S1 At-S2 At-S4	AtrOLE4
	SH2	CeOLE5	CrOLE5	ClOLE5	CmOLE5 CmOLE6	RbOLE5	ND	ND	ND	ND
	SH3	CeOLE6	CrOLE6	ND	CmOLE7	RbOLE6	JeOLE5	ND	ND	ND
	SH4	ND	ND	ND	ND	ND	ND	OsOLE5	ND	AtrOLE5

At, *A. thaliana*; Atr, *A. trichopoda*; Ce, *C. esculentus*; Cl, *C. littledalei*; Cm, *C. myosuroides*; *C. rotundus*; Je, *J. effusus*; OLE, oleosin; Rb, *R. breviuscula*; Os, *O. sativa*; SH, seed high-molecular-weight; SL, seed low-molecular-weight; T, tapetum; U, universal

187 to 679 bp. Additionally, *JeOLE2* in SL1 also contains one intron (133 bp) and the difference is that this intron is located before the hairpin-coding region (Fig. 3B). Since all *oleosin* genes present in rice and *A. trichopoda* are intronless (Supplementary Table S1), species or lineage-specific gain of these introns could be speculated.

Structural divergence among Cyperaceae and Juncaceae oleosins was also uncovered via analyzing conserved motifs. Among 15 motifs identified using MEME, Motifs 1, 2, 3, 5, 6, and 8 belong to the oleosin domain: Motif 1 is broadly distributed; Motif 2 is present in most orthogroups with the exception of SH3 that is placed by Motifs 5 and 8; and Motif 3 is present in most orthogroups with the exception of JeOLE3 and several members of SL1 (CrOLE2, ClOLE2, CmOLE2, and RbOLE2) that are placed by Motif 6. Motif 9 includes the partial sequence of the C-terminal AAPGA, which was characterized as the hallmark for Clade U (Huang and Huang 2015; Zou et al. 2022a). In contrast, little is known about other motifs: Motif 4 is widely present in SH1, SH2, and SH3, though it is replaced by Motif 7 in CeOLE6 and CrOLE6; Motif 7 is widely present in SL1 as well as two SL2 members, i.e., CeOLE3 and CrOLE3; Motif 14 is only present in CeOLE5 and CrOLE5; Motif 8 is only present in CeOLE1 and CrOLE1; Motif 11 is U-specific, though it is absent from JeOLE1; Motif 12 is SH1-specific, whereas Motif 10 is SH2-specific; Motif 13 is only present in CeOLE4 and CrOLE4 (Fig. 3C).

Global expression profiling revealed a tuber-predominant expression pattern of *CeOLE* genes

To uncover global expression profiles of *CeOLE* genes, nine tissues/developmental stages were investigated, i.e., two stages of developmental leaf (i.e. young and mature), sheath, root, rhizome, shoot apex, and three stages of developmental tuber (i.e. 40, 80, and 120 DAS). As shown in Fig. 4A, the total *CeOLE* transcripts were most abundant in tuber, peaking at 80 DAS, which is 2.44 and 1.37 folds more than 40 and 120 DAS, respectively. The average of total transcripts in three stages of developmental tuber is 31.54, 54.88, 96.65, 188.55, 195.45, and 690.70 folds more than that in root, sheath, young leaf, rhizome, shoot apex, and mature leaf, respectively, in striking contrast to seed-preferential expression of most *oleosin* genes in rice (Supplementary Fig. S2). In most tissues, *CeOLE2* in the SL1 group and *CeOLE5* in the SH2 group represent two major isoforms, though the transcripts of *CeOLE1* in the U1 group were also abundant in non-tuber tissues. Compared with shoot apex, the expression of *CeOLE5* was significantly up-regulated in young leaf, whereas the majority of *CeOLE* genes were down-regulated in mature leaf relative to young leaf. Interestingly, significantly higher abundance of *CeOLE5* was observed in sheath than leaf. Despite the low expression of *CeOLE3*, its pattern is similar to *CeOLE6*, which increased along with tuber development. *CeOLE4* transcripts also peaked at 120 DAS, but a remarkable drop was observed at 80 DAS; by contrast, *CeOLE2* and *-5* transcripts peaked at 80 DAS, and more transcripts were found at 120 DAS relative to 40 DAS (Fig. 4A and Supplementary Table S6).

CeOLE transcripts in tubers were considerably more abundant than that of purple nutsedge

Despite sharing a very close genetic relationship with tigernut, purple nutsedge accumulates few oil in its tubers, i.e. 2.5% vs 25.8% (Ji et al. 2021; Niemeyer et al. 2022), prompting us to compare the expression patterns of *oleosin* genes

Table 2 Evolutionary rate of *oleosin* homologs in tigernut, purple nutsedge, *C. littledalei*, *C. myosuroides*, *R. breviuscula*, and *J. effusus*

Species	Gene 1	Gene 2	Identity	*Ka*	*Ks*	*Ka*/*Ks*
Tigernut	*CeOLE2*	*CeOLE3*	60.8	0.2313	51.8549	0.0045
	CeOLE4	*CeOLE5*	63.0	0.2698	8.7435	0.0309
Purple nutsedge	*CrOLE2*	*CrOLE3*	60.4	0.2181	9.4525	0.0231
	CrOLE4	*CrOLE5*	62.6	0.2778	10.5926	0.0262
C. littledalei	*ClOLE2*	*ClOLE3*	57.5	0.2750	10.0150	0.2750
	ClOLE4	*ClOLE5*	61.7	0.3096	7.4242	0.0417
C. myosuroides	*CmOLE2*	*CmOLE3*	52.4	0.2942	8.4319	0.0349
	CmOLE4	*CmOLE5*	62.0	0.2824	9.7159	0.0291
R. breviuscula	*RbOLE2*	*RbOLE3*	58.1	0.2110	21.4871	0.0098
	RbOLE4	*RbOLE5*	64.7	0.2525	5.2337	0.0482
J. effusus	*JeOLE2*	*JeOLE3*	59.2	0.2442	11.4773	0.0213
Tigernut-purple nutsedge	*CeOLE1*	*CrOLE1*	97.7	0.0063	0.0692	0.0916
	CeOLE2	*CrOLE2*	93.8	0.0386	0.0954	0.4052
	CeOLE3	*CrOLE3*	93.1	0.0276	0.1869	0.1474
	CeOLE4	*CrOLE4*	96.3	0.0030	0.1370	0.0219
	CeOLE5	*CrOLE5*	99.0	0.0028	0.0322	0.0882
	CeOLE6	*CrOLE6*	97.4	0.0067	0.0783	0.0858
Tigernut-*C. littledalei*	*CeOLE1*	*ClOLE1*	77.1	0.1025	1.1546	0.0888
	CeOLE2	*ClOLE2*	73.7	0.0537	0.9316	0.0576
	CeOLE3	*ClOLE3*	83.3	0.0572	0.6228	0.0918
	CeOLE4	*ClOLE4*	81.6	0.0514	0.8044	0.0639
	CeOLE5	*ClOLE5*	73.0	0.1694	0.9989	0.1696
Tigernut-*C. myosuroides*	*CeOLE1*	*CmOLE1*	78.0	0.0935	1.1054	0.0845
	CeOLE2	*CmOLE2*	77.7	0.0842	0.8801	0.0956
	CeOLE3	*CmOLE3*	82.6	0.0675	0.6743	0.1001
	CeOLE4	*CmOLE4*	81.0	0.0577	0.8319	0.0694
	CeOLE5	*CmOLE5*	73.5	0.1671	0.9976	0.1675
	CeOLE6	*CmOLE6*	72.8	0.1253	1.1866	0.1056
Tigernut-*R. breviuscula*	*CeOLE1*	*RbOLE1*	81.2	0.0446	1.0507	0.0425
	CeOLE2	*RbOLE2*	79.3	0.0977	0.9855	0.0992
	CeOLE3	*RbOLE3*	80.1	0.0786	0.8019	0.0980
	CeOLE4	*RbOLE4*	78.3	0.0740	1.0158	0.0728
	CeOLE5	*RbOLE5*	72.0	0.1438	1.6680	0.0862
	CeOLE6	*RbOLE6*	73.8	0.1353	1.0504	0.1288
Tigernut-*J. effusus*	*CeOLE1*	*JeOLE1*	75.7	0.1169	1.8998	0.0615
	CeOLE2	*JeOLE2*	66.7	0.1678	10.7315	0.0156
	CeOLE3	*JeOLE3*	69.4	0.1541	2.5115	0.0614
	CeOLE4	*JeOLE4*	71.5	0.0929	10.7966	0.0086
	CeOLE6	*JeOLE5*	62.2	0.1989	4.0698	0.0489

Ce, *C. esculentus*; Cl, *C. littledalei*; Cm, *C. myosuroides*; *C. rotundus*; Je, *J. effusus*; Ka, nonsynonymous substitution rate; Ks, synonymous substitution rate; OLE, oleosin; Rb, *R. breviuscula*

during tuber development of these two contrasting species. As shown in Fig. 4B, among three stages profiled, i.e. 20, 50, and 90 DAI, *CeOLE* transcripts were considerably more abundant than that of *CrOLE* genes, varying from tens to thousands folds. In contrast to the predominant expression of two *CeOLE* genes (i.e. *CeOLE2* and *-5*), major transcripts in purple nutsedge were contributed by three isoforms, i.e., *CrOLE2*, *CrOLE1*, and *CrOLE6* (accounting for about 90.0%) in order. Moreover, their expression was not much correlated with tuber development except for *CrOLE2* and *CrOLE5* that was visibly up-regulated at 50 DAI. In contrast, transcripts of most *CeOLE* genes gradually increased along with tuber development. Whereas total *CrOLE* transcripts peaked at 50 DAI, *CeOLE* transcripts peaked at 90 DAI and relatively high-level expression started even at 20 DAI (Fig. 4B and Supplementary Table S7).

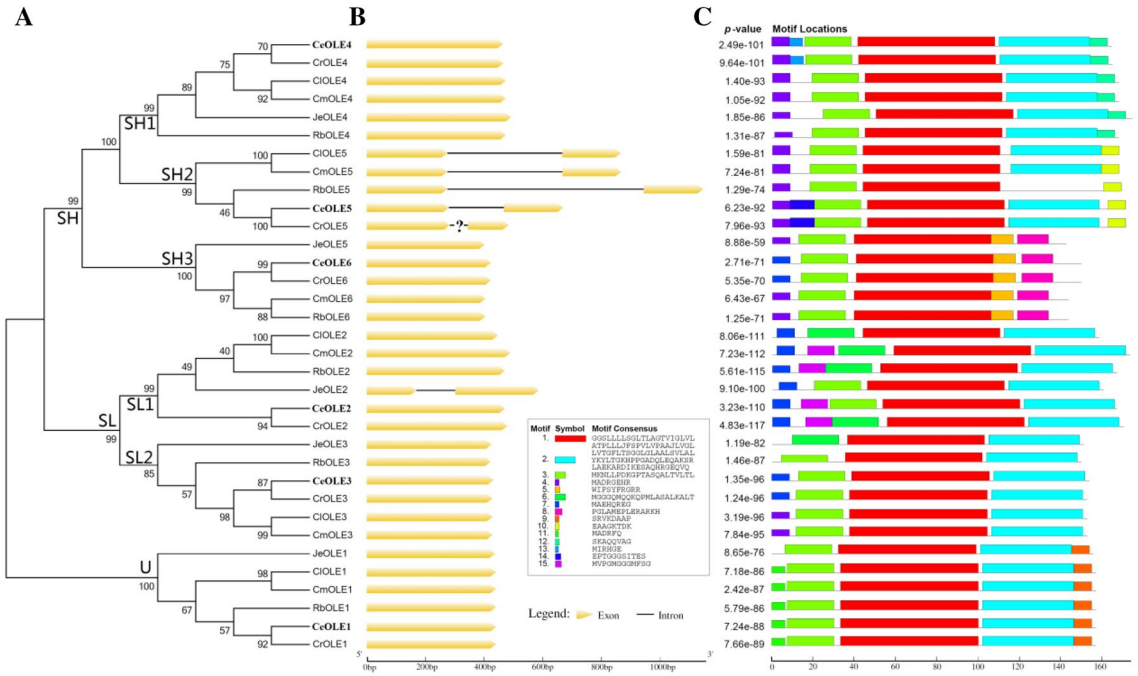

Fig. 3 Structural and phylogenetic analysis of the *oleosin* family in tigernut, purple nutsedge, *C. littledalei*, *C. myosuroides*, *R. breviuscula*, and *J. effuses*. **A** Shown is an unrooted phylogenetic tree resulting from full-length oleosins with MEGA6 (maximum likelihood method and bootstrap of 1,000 replicates), where the distance scale denotes the number of amino acid substitutions per site and the name of each clade is indicated next to the corresponding group. **B** Shown are the exon–intron structures. "?" represents the unknown length. **C** Shown is the distribution of conserved motifs among oleosins, where different motifs are represented by different color blocks as indicated and the same color block in different proteins indicates a certain motif. (Ce, *C. esculentus*; Cl, *C. littledalei*; Cm, *C. myosuroides*; Cr, *C. rotundus*; Je, *J. effusus*; OLE, oleosin; Rb, *R. breviuscula*; SH, seed high-molecular-weight; SL, seed low-molecular-weight; T, tapetum; U, universal)

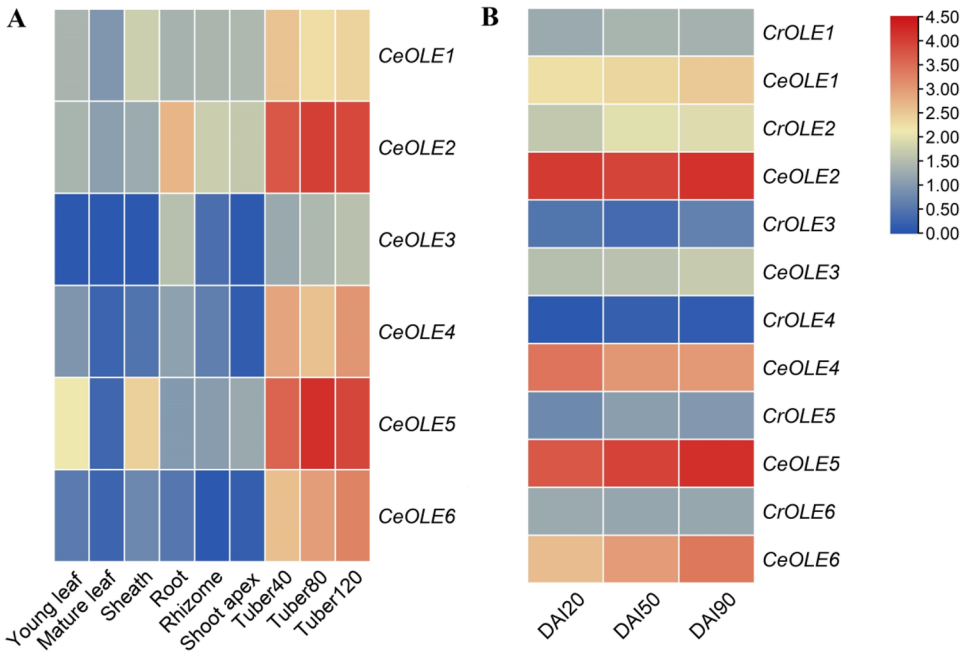

Fig. 4 Expression profiles of *oleosin* genes in tigernut and purple nutsedge. **A** Tissue-specific expression profiles of *CeOLE* genes. Tuber40, Tuber80, and Tuber120 represent tubers of 40, 80 and 120 DAS. **B** Expression profiles of *CeOLE* and *CrOLE* genes during tuber development. Color scale represents FKPM normalized $\log_{10}$ transformed counts where red indicates low expression and blue indicates high expression. (Ce, *C. esculentus*; Cr, *C. rotundus*; DAI, days after tuber initiation; DAS, days after sowing; FKPM, fragments per kilobase of exon per million fragments mapped; OLE, oleosin)

TAG accumulation and *CeOLE* mRNA/protein profiles during tuber development

In tigernut, it has been well established that TAGs gradually increase along with tuber development, peaking at the maturity (Jin et al. 2010; Turesson et al. 2010; Ji et al. 2021; Wang et al. 2021). In the present study, the whole growth period observed was about 85 d, and new tubers began to appear from approximately four weeks after shoot emergence. Visible tubers collected in this study were defined as the first stage, i.e. 1 DAI, and the mean dry mass per tuber was about 2.8 mg. In later stages of development, the dry matter increased gradually, peaking at the maturity of 35 DAI with approximately 1264.4 mg/tuber (Fig. 5A). A total of six swelling stages were collected, i.e. 3, 5, 10, 15, 20, and 25 DAI, where the former five stages were characterized as white in appearance. At 25 DAI, tubers began to turn light brown and their size had reached the maximum. In contrast, tubers at 35 DAI had totally matured and were characterized as hard and dark brown in appearance. The TAG content at above eight stages was also measured, and results showed that TAGs were not detected until 5 DAI, i.e., 5.1% of dry weight. Later, the TAG content slowly increased to 8.4% at 20 DAI, followed by the fast increase to 20.6% and 34.3% at 25 and 35 DAI, respectively (Fig. 5B).

To reveal the correlation between gene expression and TAG accumulation, the transcript levels of *CeOLE* genes in different developmental tubers were further checked using qRT-PCR. As shown in Fig. 6, the expression of most *CeOLE* genes is positively correlated with TAG accumulation during tuber development. At 1 DAI, *CeOLE* genes were usually lowly expressed with the exception of *CeOLE1* whose transcripts were more abundant than that at 3 and 5 DAI. Later, most genes were significantly up-regulated, especially at two late stages, i.e., 25 and 35 DAI. Consistent with transcriptional profiling as described above, *CeOLE2* and *-5* represent two major isoforms with considerably lower Ct values, supporting expression divergence with their recent paralogs *CeOLE3* and *CeOLE4*, respectively. In contrast, despite the relatively low expression, *CeOLE6* and *CeOLE4* were shown to be two most up-regulated genes during tuber maturity. It is worth noting that, a sudden drop

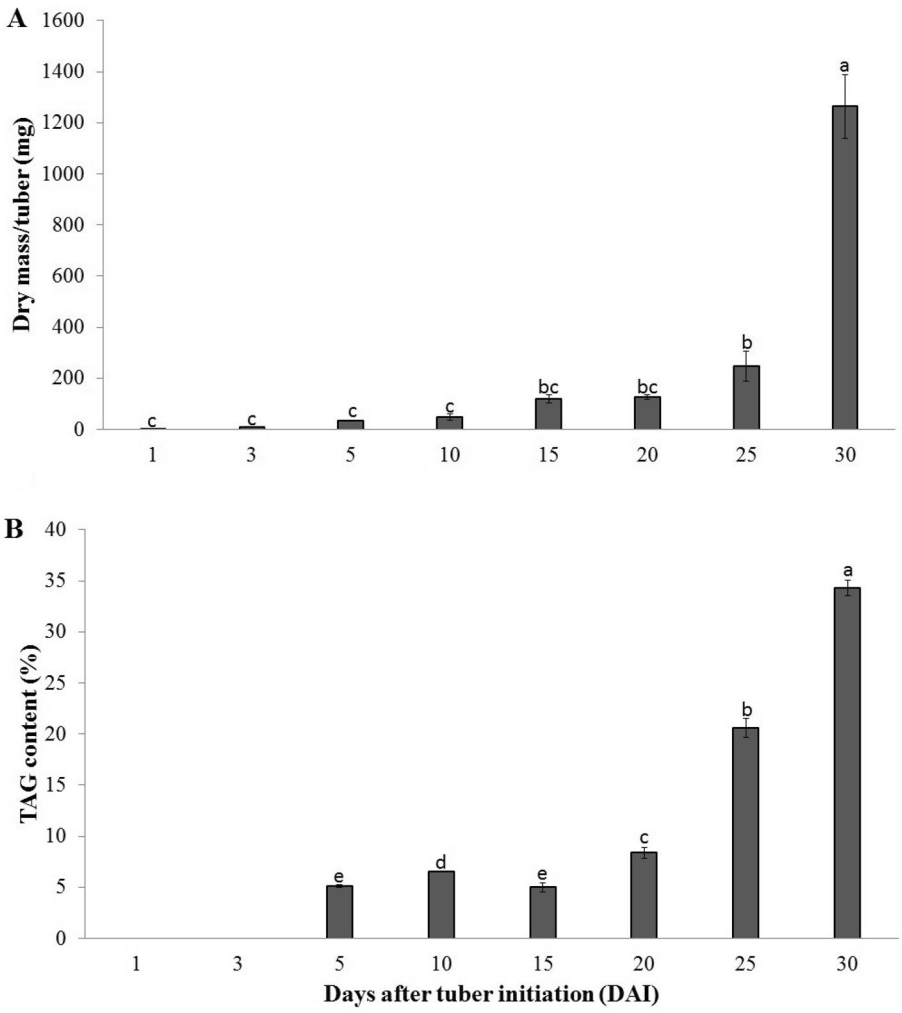

Fig. 5 Dry mass (**A**) and TAG (**B**) accumulation in developing tigernut tubers from 1 to 35 DAI. Bars indicate SD ($N \geq 3$) and lowercase letters indicate difference significance tested following Duncan's one-way multiple-range post hoc ANOVA ($P < 0.05$). (DAI, days after tuber initiation; TAG, triacylglycerol)

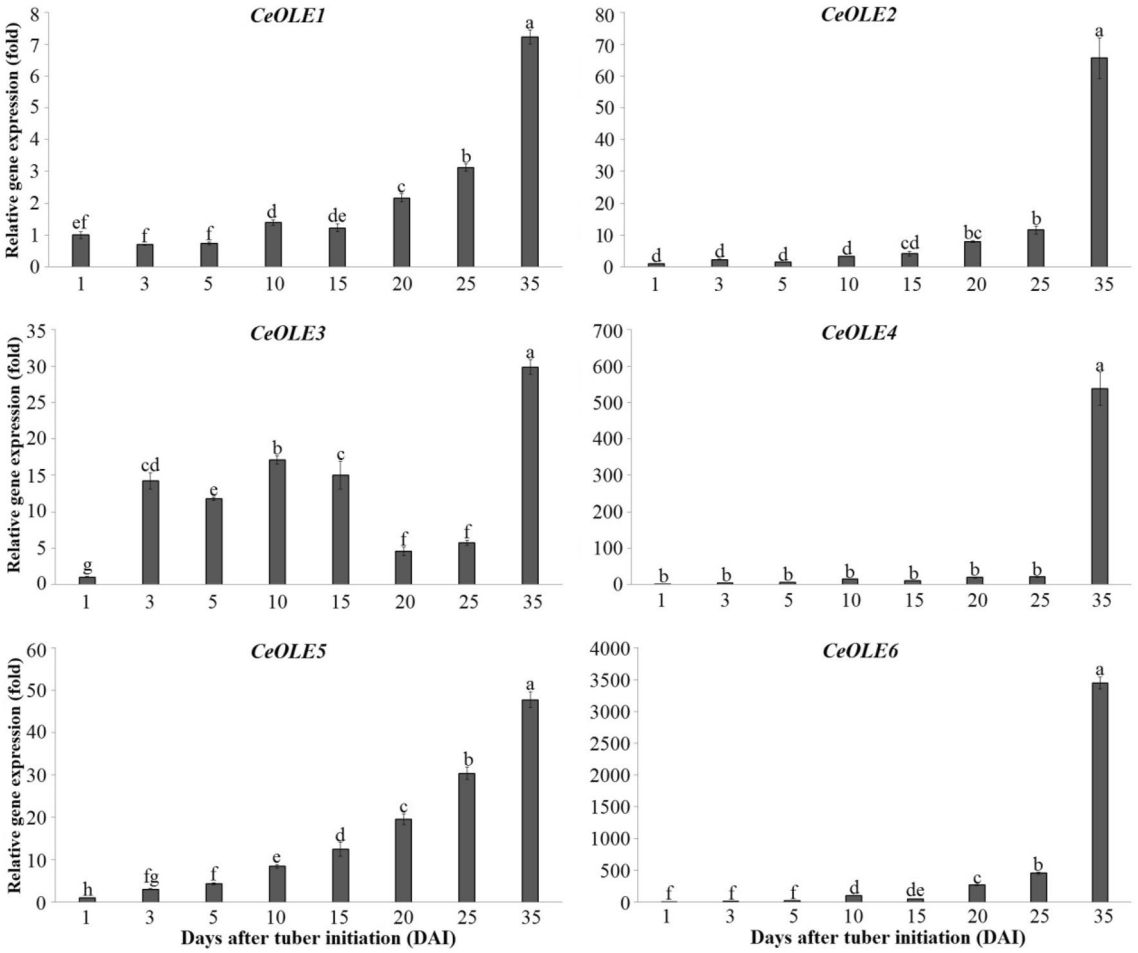

Fig. 6 Expression profiles of *CeOLE* genes during tuber development. Bars indicate SD ($N=3$) and lowercase letters indicate difference significance tested following Duncan's one-way multiple-range post hoc ANOVA ($P<0.05$). (Ce, *C. esculentus*; DAI, days after tuber initiation; OLE, oleosin)

of gene expression was observed for *CeOLE6* and *CeOLE1* at 15 DAI, when a drop of TAG content was also observed. The reason for this needs to be further studied.

Considering that protein abundance is not always in agreement with the transcript level and *oleosin* genes shall function at the protein level, we therefore first took advantage of available proteomic data to identify and quantify oleosins in both tigernut and purple nutsedge. As shown in Fig. 7A, all six CeOLE proteins were identified in LD-enriched fractions, though their abundances were highly variable. In total protein extracts, however, only four members, i.e., CeOLE1, CeOLE2, CeOLE5, and CeOLE6, were identified in freshly harvested, dried, rehydrated for 48 h, and sprouted tubers, in contrast to none in roots and leaves. As expected, protein abundance in total protein extracts was considerably less than that in LD-enriched fractions. Notably, despite the presence of six *CrOLE* genes, only the protein of *CrOLE1* was identified in total proteins of freshly harvested tubers, which may be due to less sensitivity of proteomic techniques and correspond to relatively low levels of their transcripts in tubers as described above (Fig. 4B). To further uncover the protein dynamics during tuber development, two dominant isoforms (i.e. CeOLE2 and -5) were profiled in three representative stages, i.e. 5 DAI, 20 DAI, and 35 DAI, where 5 DAI was selected as the first stage for its clear TAG accumulation as described above (Fig. 5B). As shown in Fig. 7B, three to six and two to four fold increase was observed for CeOLE2 and -5, respectively. Their increased percentage is more in accordance with TAG accumulation (Fig. 5B), but far less than the transcript (Fig. 6A).

Protein interaction and subcellular localization of CeOLE2 and -5

As described above, at both transcription and protein levels, *CeOLE2* and *-5* represent two dominant isoforms. Their co-expression and high abundance in small LDs suggest that they may interact with each other. For this purpose, BiFC

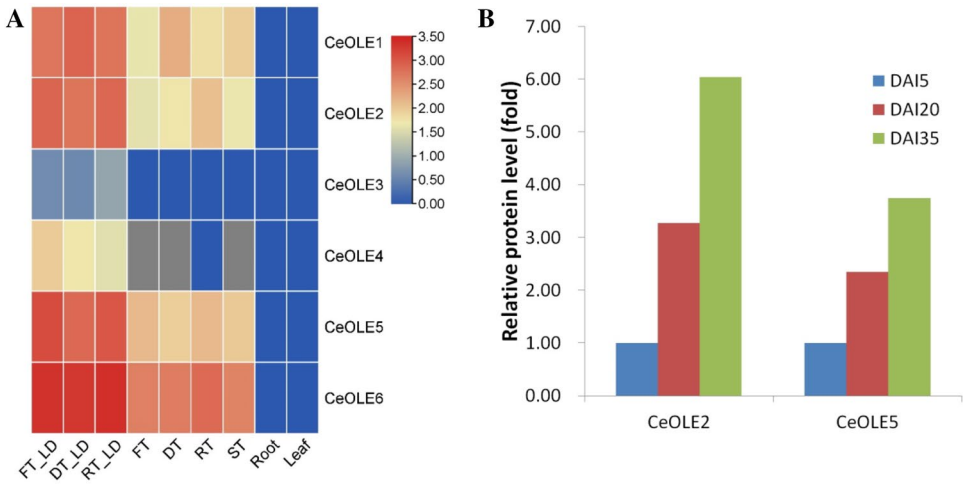

Fig. 7 Relative protein abundance of *CeOLE* genes in different tissues (**A**) and stages of tuber development (**B**). Color scale represents intensity normalized $\log_2$ transformed relative quantitative values where red indicates low expression and blue indicates high expression. (Ce, *C. esculentus*; DAI, days after tuber initiation; DT, dried tubers; FT, freshly harvested tubers; LD, lipid droplet; OLE, oleosin; RT, rehydrated tubers for 48 h; ST, sprouted tubers)

analysis was carried out using *A. tumefaciens*-mediated infiltration of tobacco leaves (Qiao et al. 2022a). As shown in Fig. 8, our results indeed supported protein interaction between CeOLE2 and -5. Moreover, homologous interaction was also observed, implying that oleosins are more likely to function in homo and heteromultimers. Despite the well-known LD-localization of oleosins (Yee et al. 2021; Niemeyer et al. 2022), to our surprise, CeOLE2 and -5 were shown to locate not only in LDs (highly similar to that reported by Yee et al. 2021) but also the ER when transiently overexpressed in tobacco leaves of the BiFC experiment (Fig. 8). To confirm the result, an ER marker RFP-HDEL described before (Gong et al. 2021) was also used for subcellular localization analysis. As shown in Fig. 9, in the ER, fluorescence signals of CeOLE2-EGFP and CeOLE5-EGFP were highly coincided with RFP-HDEL, supporting their ER-localization.

Overexpressing CeOLE2 and -5 in tobacco leaves

Due to the lack of an efficient genetic transformation platform for tigernut, roles of *CeOLE2* and *-5* in oil accumulation of vegetative tissues were investigated via transiently overexpressing in tobacco leaves, which has been widely employed to study genes involved in oil regulation (Grimberg et al. 2015; Yee et al. 2021; Xu et al. 2022; Kim et al. 2023). As shown in Fig. 10A, transcripts of *CeOLE2* and *-5* were detected even at 1 d after infiltration, and then steadily increased for 2.74–3.17 and 28.71–50.33 folds at two later time points, i.e., 3 d and 5 d, respectively. The TAG contents of transformed leaves were also examined. As for controls that were transformed with the empty vector, the TAG content was about 3.57 mg/g, in contrast, those of transgenic leaves increased 1.52–2.33 and 1.52–2.15 folds for *CeOLE2* and *-5* at three time points (1 d, 3 d, and 5 d) examined, respectively. Interestingly, both of them were shown to peak at 3 d after infiltration (Fig. 10B). The result supported a role of these two genes in oil accumulation of vegetative tissues.

Discussion

As the rapid increase of world population and vegetable oil consumption, the huge demand for edible oil has put pressure on the supply by traditional oil crops, which predominantly accumulate high amounts of TAGs in their seeds (Board et al. 2022). Although plant vegetative tissues usually do not produce significant levels of TAGs, they have the capacity for their synthesis, storage, and metabolism, providing an opportunity to create alternative resources for increasing overall plant oil production (Xu and Shanklin 2016). Nevertheless, our knowledge on oil metabolism and regulation are mainly from arabidopsis and related oilseed crops (Bates et al. 2013; Xu and Shanklin 2016). Exploring new resources and characterizing key genes associated with oil accumulation in vegetative tissues are of particular interest.

Expansion of the *oleosin* family in tigernut was contributed by WGD and dispersed duplication, which were shown to be lineage-specific

As a rare example accumulating high levels of TAGs in the underground tubers, tigernut has been emerging as a novel oil crop and an idea model to study the mechanism of oil accumulation in vegetative tissues (Jin et al. 2010; Turesson et al. 2010; Xu et al. 2022; Zhao et al. 2023). Like seeds of oil crops, proteome analysis of LD-enriched fractions indicated that LDs of tigernut tubers are largely coated by oleosins (Niemeyer et al. 2022), in striking contrast to LDs in leaves, roots, and the mesocarp of avocado (*Persea americana*) that are mainly enclosed by lipid droplet-associated proteins (LDAPs) or small rubber particle proteins (SRPPs)

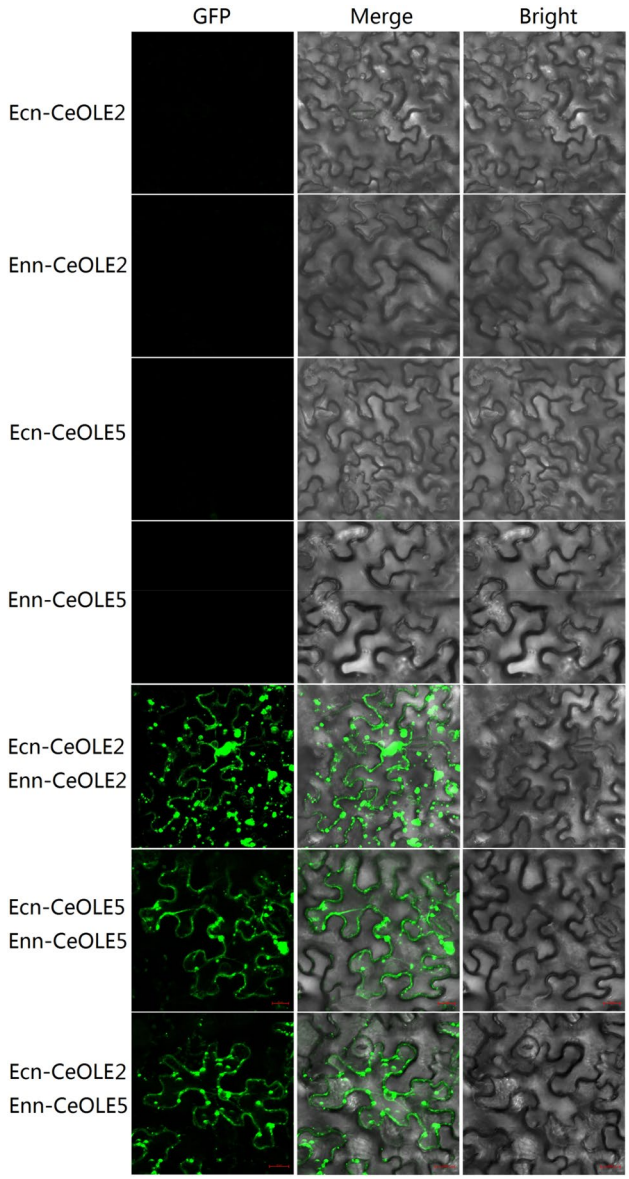

Fig. 8 BiFC-based protein interaction of CeOLE2 and CeOLE5 in tobacco leaves. (Ce, *C. esculentus*; OLE, oleosin)

(Horn et al. 2013; Kretzschmar et al. 2020; Guzha et al. 2023).

To improve our knowledge on roles of oleosins in vegetative tissues, in this study, a comprehensive characterization of the *oleosin* family was conducted in tigernut and six members identified represent three out of six previously described clades, i.e., U (1), SL (2), and SH (3), which is consistent with that reported in other monocots (Liu et al. 2012; Huang and Huang 2015; Ojha et al. 2021). Nevertheless, despite possessing equal members with most Poaceae species (e.g. six in rice), the family composition and evolution pattern were shown to be different. In rice that has been proven to experience three rounds of WGDs (named τ, σ, and ρ) after monocot-eudicot split (Jiao et al. 2014), the *oleosin* family is composed by two members for each clade: two U members, i.e., *OsOLE1* and *OsOLE4*, were derived from the Poaceae-specific ρ WGD; two SL members, i.e., *OsOLE3* and *OsOLE6*, were resulted from dispersed duplication (Supplementary Table S1); and they constitute four out of seven orthogroups proposed in this study, i.e., U, SL1, SH1, and SH4 (Table 1). Since these four orthogroups are also present in *A. trichopoda*, a basal angiosperm (Amborella Genome Project 2013), their early divergence before monocot-eudicot split and lineage-specific contraction in Cyperaceae and Juncaceae could be speculated. In contrast, *CeOLE* genes constitute six orthogroups, i.e., U, SL1, SL2, SH1, SH2, and SH3, three of which were shown to be absent from rice, arabidopsis, and *A. trichopoda*, implying their recent origin or lineage-specific contraction in rice. To address this issue, genome-wide identification of *oleosin* genes was also performed in representative species of Cyperaceae and Juncaceae. The wide presence of SL2, SH2, and SH3 in tested Cyperaceae species, i.e., purple nutsedge, *C. myosuroides*, and *R. breviuscula*, implies their divergence before the radiation of Cyperaceae. Since both SL2 and SH3 homologs have already been present in *J. effuses*, their generation could be dated back to sometime before Cyperaceae-Juncaceae divergence. Moreover, the location of SL1 and SL2 in syntenic blocks supports their WGD-derivation, which is more likely to be shared by Cyperaceae and Juncaceae or the recent WGD as described in *C. littledalei* (Can et al. 2020). In contrast, SH3 and SH2 were characterized as dispersed repeats of SH1, which may be respectively generated sometime before or after the recent WGD via yet unknown mechanisms. The evolution pattern is also different from arabidopsis that experienced three WGDs (named γ, β, and α) after monocot-eudicot split (Bowers et al. 2003), the expansion (in all orthogroups) of whose family was contributed by WGDs (β, 1; α, 3), tandem (5), proximal (1), and transposed duplications (1) (Supplementary Table S1).

Evolution of *CeOLE* genes was driven by divergence of gene structures and conserved motifs

Although three clades of oleosins have been established in monocots (Liu et al. 2012; Huang and Huang 2015), their subclassification is yet to be resolved. In this study, classification of six *CeOLE* genes into six groups is supported not only by exon–intron structures but also by conserved motifs. Generally, *oleosin* genes are intronless. However, gain of certain introns has been reported in some lineages, e.g., Euphorbiaceae, Brassicaceae, Cyperaceae, and Juncaceae (Huang and Huang 2015; Jia et al. 2022; Zou et al. 2022a; This study). In arabidopsis, 88.24% of *oleosin* genes were shown to possess one to two introns, which appear in

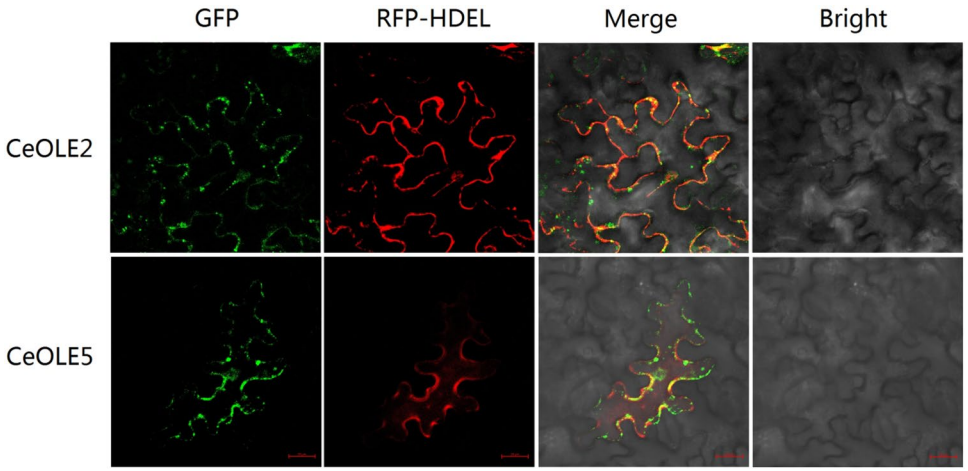

Fig. 9 Subcellular localization analysis of CeOLE2 and CeOLE5 in tobacco leaves. (Ce, *C. esculentus*; OLE, oleosin)

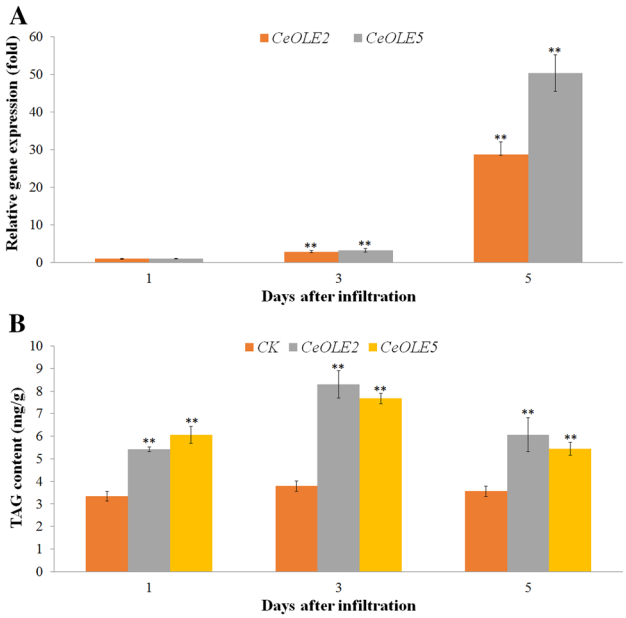

Fig. 10 Transcript (**A**) and TAG (**B**) increase in *CeOLE2* and *CeOLE5*-overexpressing tobacco leaves. Bars indicate SD ($N=3$) and "**" indicate difference significance tested following Duncan's one-way multiple-range post hoc ANOVA ($P<0.01$). (Ce, *C. esculentus*; OLE, oleosin; TAG, triacylglycerol)

different positions (Zou et al. 2022a). Position of the intron found in Cyperaceae species is similar to that reported in Euphorbiaceae species (Zou et al. 2022a), which is different from that found in *JeOLE2*, a SL1 member. Thereby, SH2 may differ from SH1 with the presence of one intron.

Different groups may also harbor group-specific conserved motifs. In this study, without any exception, the U clade was shown to include Motif 9 or the conserved AAPGA motif, which was characterized as the hallmark for this clade before (Huang and Huang 2015; Zou et al. 2022a). SH1 and SH2 differ from other groups with the presence of a putative C-terminal insertion of 18 AA as widely described in the SH clade (Tzen et al. 1990; Huang and Huang 2015; Jia et al. 2022; Zou et al. 2022a). Besides the presence of one conserved intron, SH2 also differs from SH1 with the substitution of Motif 12 by Motif 10 at the C termini. SH3 differs from other groups with the substitution of Motif 2 by Motifs 5 and 8. These results imply possible function divergence of different groups.

CeOLE genes have evolved to predominantly express in oil-rich tubers and exhibit seed-like accumulation with TAGs during tuber development

Generally, *oleosin* genes are preferentially expressed in seeds of oil crops, especially in maturing seeds with high levels of TAGs and abundant LDs (Kim et al. 2002; Huang and Huang 2015; Zhang et al. 2019; Jia et al. 2022; Zou et al. 2022a). In arabidopsis, rapeseed, and soybean, oleosin abundances were shown to be negatively correlated with the LD size and positively related to the oil content of seeds (Siloto et al. 2006; Hu et al. 2009; Zhang et al. 2019). Moreover, overexpression of *oleosin* genes could increase the seed oil content in arabidopsis, rice, and soybean (Liu et al. 2013; Zhang et al. 2019; Ojha et al. 2021; Yuan et al. 2021). Since tigernut rarely set seeds, we are not able to examine the TAG accumulation and expression profiles of *CeOLE* genes during seed development. Instead, transcriptional profiling of several main tissues (i.e., leaf, sheath, root, rhizome, shoot apex, and tuber) showed that most *CeOLE* genes were predominantly expressed in the tuber, coinciding with high amounts of TAGs produced by this special tissue (Jin et al. 2010; Turesson et al. 2010; Codina-Torrella et al. 2015; This study). In fact, tuber-predominant expression of *CeOLE* genes appears to be tigernut-specific, co-opting with the LD/TAG accumulation but not the tuber tissue itself. Evidences are as follows: Firstly, as a close relative to tigernut that may diverge as late as 0.3–12 million

years ago (MYA) (Niemeyer et al. 2022; Xiao et al. 2022; Zou et al. 2023a), purple nutsedge produces tubers with high amounts of starch instead of TAGs (Stoller and Weber 1975; Ji et al. 2021); secondly, despite the presence of six *CrOLE* genes, their transcripts in tubers especially at late stages were considerably less than that of *CeOLE* genes; thirdly, despite the detectability of all six CeOLE proteins in LD proteomes (Niemeyer et al. 2022), four of them (i.e. CeOLE1, CeOLE2, CeOLE5, and CeOLE6) were also identified in total proteins of freshly harvested tubers, in contrast to a single one (i.e. CrOLE1) detected in freshly harvested tubers of purple nutsedge; fourthly, *CrOLE1* belongs to the U clade whose homologs such as *CeOLE1* was universally expressed in most tissues including leaf, sheath, root, rhizome, and shoot apex examined in this study; finally, *CeOLE* genes were lowly expressed in early stages of developmental tuber and transcripts/proteins gradually increased along with TAG accumulation during later development, which is consistent with the accumulating dynamics of LDs reported in tigernut (Jin et al. 2010; Turesson et al. 2010; Wang et al. 2021). Nevertheless, the mechanism underlying is still to be addressed. One possible cause may be the co-opting master regulator WRINKLED1 (WRI1) encoded by *CeWRI1*, whose transcripts were also shown to positively correlate with TAG accumulation during tuber development (Xu et al. 2022). However, genes encoding other master regulators homologous to FUSCA3 (FUS3), LEAFY COTYLEDON1 (LEC1), LEAFY COTYLEDON2 (LEC2), and ABSCISIC ACID INSENSITIVE3 are rarely expressed in tubers (Zou et al. 2021), implying tuber-specific regulatory of oil accumulation in tigernut.

Oleosins may function in homo and heteromultimers

Among six clades (i.e. P, U, SL, SH, T, and M) of oleosins described, SL and SH represent two clades that are highly abundant in seeds of angiosperm (Huang and Huang 2015). Despite wide occurrence of species or lineage-specific expansion of these two clades, generally only one from each clade is active and they are usually in an approximately 1:1 ratio (Tzen et al. 1990; Huang and Huang 2015; Zou et al. 2022a), implying possible interaction between SL and SH oleosins. In tigernut, despite recent origin of SL and SH paralogs, i.e. *CeOLE2*/*-3* and *CeOLE4*/*-5*, apparent expression divergence was observed and *CeOLE2*/*-5* have evolved to be two dominant isoforms in oil-rich tubers. As expected, according to our BiFC analysis, CeOLE2 and -5 could indeed interact with each other. Moreover, strong homologous interaction could also be detected for CeOLE2 and -5, supporting that oleosins may function in homo and heteromultimers. To the best of our knowledge, this is the first experimental evidence for oleosin multimerization. Additionally, both BiFC and subcellular localization analyses suggest that CeOLE2 and -5 are located not only in LDs but also the ER when transiently overexpressed in tobacco leaves. Their LD-localization is in accordance with proteome analysis of LD-enriched fractions (Niemeyer et al. 2022) as well as subcellular localization analyses performed in other species (Abell et al. 1997; Huang and Huang 2017; Yee et al. 2021). In contrast, their retention in ER is more likely due to overexpression resulting in mass synthesis of oleosins in ER and limited LDs present in the leaf tissue (Abell et al. 1997; Huang and Huang 2017).

Overexpression of *CeOLE* genes could improve oil accumulation in leaves

As discussed above, tuber-specific activation of *CeOLE* genes is more likely to be a key factor determining high levels of oil accumulation in tigernut tubers, in accordance with artificial selection of soybean *OLEO1* that resulted in the high level of transcription and increased seed oil accumulation (Zhang et al. 2019). Nevertheless, direct functional evidence is lacking for *CeOLE* genes. Since the genetic transformation system has not been well established in tigernut, a method for transiently overexpressing in tobacco leaves was used for the purpose. As the main tissue for photosynthesis, under normal conditions, leaves rarely accumulates LDs and oleosins (Kretzschmar et al. 2020; Niemeyer et al. 2022). However, they have the capacity for oil biosynthesis and overexpressing oil-related genes such as *WRI1* could increase the TAG content in transgenic leaves, just like that observed in transgenic seeds of arabidopsis, rice, and soybean (Liu et al. 2013; Grimberg et al. 2015; Zhang et al. 2019; Ojha et al. 2021; Yuan et al. 2021; Xu et al. 2022). As expected, transiently overexpressing two dominant isoforms (i.e., *CeOLE2* and *-5*) in tobacco leaves could significantly increase the TAG content by 1.52–2.33 folds. The increased folds are comparable to that of *CeWRI1*-overexpressing leaves, however, the trend is different: for both *CeOLE2* and *-5*, the TAG content peaked at 3 d after infiltration, in contrast to 5 d for *CeWRI1* (Xu et al. 2022). The underlying mechanism still needs to be studied and one possible reason may be due to their inherent characteristics: oleosins are structural proteins that mainly function in LD formation and stabilization, whereas WRI1 is a master regulator of genes involved in oil biosynthesis (Grimberg et al. 2015; Kong et al. 2019; Qiao et al. 2022b; Xu et al. 2022).

Conclusions

To our knowledge, this is the first genome-wide characterization of the *oleosin* family in tigernut, a unique Cyperaceae plant producing TAGs in its underground tubers.

Six members identified represent three clades (i.e. U, SL and SH) or six out of seven orthogroups proposed in this study, i.e., U, SL1, SL2, and SH1–3. Expansion of Clades SL and SH appears to be lineage-specific, contributed by WGD and dispersed duplication, respectively. Evolution of *CeOLE* genes was driven by divergence of gene structures, conserved motifs, and expression profiles. *CeOLE* genes have evolved to predominantly express in oil-rich tubers and exhibit seed-like accumulation (at both mRNA and protein levels) with TAGs during tuber development. Roles of *CeOLE* genes in oil accumulation of vegetative tissues were confirmed via overexpressing in tobacco leaves. Moreover, homologous and heterologous interactions of CeOLE proteins were first presented in this study. These findings provide insights into lineage-specific family evolution and putative roles of *oleosin* genes in oil accumulation of underground tubers, which facilitate further genetic improvement for tigernut.

Supplementary Information The online version contains supplementary material available at https://doi.org/10.1007/s00299-023-03066-x.

Acknowledgements The authors appreciate those contributors who make related genome and transcriptome data accessible in public databases.

Author contribution statement The study was conceived and directed by Zhi Zou. All the experiments and analyses were directed by Zhi Zou and carried out by Zhi Zou, Yujiao Zheng, Zhongtian Zhang, Yanhua Xiao, Zhengnan Xie, Lili Chang, Li Zhang, and Yongguo Zhao. Zhi Zou, Li Zhang, and Yongguo Zhao wrote the paper. All the authors read and approved the final manuscript.

Funding This work was supported by the Project of Sanya Yazhou Bay Science and Technology City (SCKJ-JYRC-2022-66), China; the Central Public-interest Scientific Institution Basal Research Fund (1630052022001), China; and the National Natural Science Foundation of China (31971688), China; the Natural Science Foundation of Hainan province (320RC705), China. The funders had no role in study design, data collection and analysis, decision to publish, or preparation of the manuscript.

Data availability The original contributions presented in the study are included in the article/Supplementary Material, and further inquiries can be directed to the corresponding authors.

Declarations

Conflict of interest The authors declare that the research was conducted in the absence of any commercial or financial relationships that could be construed as a potential conflict of interest.

References

Abell BM, Holbrook LA, Abenes M, Murphy DJ, Hills MJ, Moloney MM (1997) Role of the proline knot motif in oleosin endoplasmic reticulum topology and oil body targeting. Plant Cell 9:1481–1493

Amborella Genome Project (2013) The *Amborella* genome and the evolution of flowering plants. Science 342:1241089

Bai X, Chen T, Wu Y, Tang M, Xu ZF (2021) Selection and validation of reference genes for qRT-PCR analysis in the oil-rich tuber crop tiger nut (*Cyperus esculentus*) based on transcriptome data. Int J Mol Sci 22:2569

Barminas JT, Maina HM, Tahir S, Kubmarawa D, Tsware K (2001) A preliminary investigation into the biofuel characteristics of tigernut (*Cyperus esculentus*) oil. Bioresour Technol 79:87–89

Bates PD, Stymne S, Ohlrogge J (2013) Biochemical pathways in seed oil synthesis. Curr Opin Plant Biol 16:358–364

Board AJ, Crowther JM, Acevedo-Fani A, Meisrimler CN, Jameson GB, Dobson RCJ (2022) How plants solubilise seed fats: Revisiting oleosin structure and function to inform commercial applications. Biophys Rev 14:257–266

Bowers JE, Chapman BA, Rong J, Paterson AH (2003) Unravelling angiosperm genome evolution by phylogenetic analysis of chromosomal duplication events. Nature 422:433–438

Brocard L, Immel F, Coulon D, Esnay N, Tuphile K, Pascal S, Claverol S, Fouillen L, Bessoule JJ, Bréhélin C (2017) Proteomic analysis of lipid droplets from *Arabidopsis* aging leaves brings new insight into their biogenesis and functions. Front Plant Sci 8:894

Can M, Wei W, Zi H, Bai M, Liu Y, Gao D, Tu D, Bao Y, Wang L, Chen S, Zhao X, Qu G (2020) Genome sequence of *Kobresia littledalei*, the first chromosome-level genome in the family Cyperaceae. Sci Data 7:175

Chen C, Chen H, Zhang Y, Thomas HR, Frank MH, He Y, Xia R (2020) TBtools: an integrative toolkit developed for interactive analyses of big biological data. Mol Plant 13:1194–1202

Codina-Torrella I, Guamis B, Trujillo AJ (2015) Characterization and comparison of tiger nuts (*Cyperus esculentus* L.) from different geographical origin: Physico-chemical characteristics and protein fractionation. Ind Crop Prod 65:406–414

De Castro O, Gargiulo R, Del Guacchio E, Caputo P, De Luca P (2015) A molecular survey concerning the origin of *Cyperus esculentus* (Cyperaceae, Poales): Two sides of the same coin (weed vs. crop). Ann Bot 115:733–745

Gong J, Tian Z, Qu X, Meng Q, Guan Y, Liu P, Chen C, Deng X, Guo W, Cheng Y, Wang P (2021) Illuminating the cells: Transient transformation of citrus to study gene functions and organelle activities related to fruit quality. Hortic Res 8:175

Grimberg Å, Carlsson AS, Marttila S, Bhalerao R, Hofvander P (2015) Transcriptional transitions in *Nicotiana benthamiana* leaves upon induction of oil synthesis by WRINKLED1 homologs from diverse species and tissues. BMC Plant Biol 15:192

Guzha A, Whitehead P, Ischebeck T, Chapman KD (2023) Lipid droplets: packing hydrophobic molecules within the aqueous cytoplasm. Annu Rev Plant Biol 74:195–223

Hofstatter PG, Thangavel G, Lux T, Neumann P, Vondrak T, Novak P, Zhang M, Costa L, Castellani M, Scott A, Toegelová H, Fuchs J, Mata-Sucre Y, Dias Y, Vanzela ALL, Huettel B, Almeida CCS, Šimková H, Souza G, Pedrosa-Harand A, Macas J, Mayer KFX, Houben A, Marques A (2022) Repeat-based holocentromeres influence genome architecture and karyotype evolution. Cell 185:3153–3168.e18

Horn PJ, James CN, Gidda SK, Kilaru A, Dyer JM, Mullen RT, Ohlrogge JB, Chapman KD (2013) Identification of a new class of lipid droplet-associated proteins in plants. Plant Physiol 162:1926–1936

Hsieh K, Huang AH (2004) Endoplasmic reticulum, oleosins, and oils in seeds and tapetum cells. Plant Physiol 136:3427–3434

Hu Z, Wang X, Zhan G, Liu G, Hua W, Wang H (2009) Unusually large oilbodies are highly correlated with lower oil content in *Brassica napus*. Plant Cell Rep 28:541–549

Huang AH (2018) Plant lipid droplets and their associated proteins: potential for rapid advances. Plant Physiol 176:1894–1918

Huang MD, Huang AH (2015) Bioinformatics reveal five lineages of oleosins and the mechanism of lineage evolution related to structure/function from green algae to seed plants. Plant Physiol 169:453–470

Huang CY, Huang AHC (2017) Unique motifs and length of hairpin in oleosin target the cytosolic side of endoplasmic reticulum and budding lipid droplet. Plant Physiol 174:2248–2260

Ji H, Liu D, Yang Z (2021) High oil accumulation in tuber of yellow nutsedge compared to purple nutsedge is associated with more abundant expression of genes involved in fatty acid synthesis and triacylglycerol storage. Biotechnol Biofuels 14:54

Jia Y, Yao M, He X, Xiong X, Guan M, Liu Z, Guan C, Qian L (2022) Transcriptome and regional association analyses reveal the effects of oleosin genes on the accumulation of oil content in *Brassica napus*. Plants (basel) 11:3140

Jiao Y, Li J, Tang H, Paterson AH (2014) Integrated syntenic and phylogenomic analyses reveal an ancient genome duplication in monocots. Plant Cell 26:2792–2802

Jin MY, Duan XQ, Zhao YG, Wei WL (2010) Primary study on laws of accumulation, distribution and transformation of dry matter in *Cyperus esculentus*. Southwest China J Agr Sci 23:475–479

Kim HU, Hsieh K, Ratnayake C, Huang AH (2002) A novel group of oleosins is present inside the pollen of *Arabidopsis*. J Biol Chem 277:22677–22684

Kim S, Lee KR, Suh MC (2023) Ectopic expression of *Perilla frutescens WRI1* enhanced storage oil accumulation in *Nicotiana benthamiana* leaves. Plants (basel) 12:1081

Kong Q, Yuan L, Ma W (2019) WRINKLED1, a "Master Regulator" in transcriptional control of plant oil biosynthesis. Plants (basel) 8:238

Kretzschmar FK, Doner NM, Krawczyk HE, Scholz P, Schmitt K, Valerius O, Braus GH, Mullen RT, Ischebeck T (2020) Identification of low-abundance lipid droplet proteins in seeds and seedlings. Plant Physiol 182:1326–1345

Langmead B, Salzberg SL (2012) Fast gapped-read alignment with Bowtie 2. Nat Methods 9:357–359

Liu Q, Sun Y, Su W, Yang J, Liu X, Wang Y, Wang F, Li H, Li X (2012) Species-specific size expansion and molecular evolution of the oleosins in angiosperms. Gene 509:247–257

Liu WX, Liu HL, le Qu Q (2013) Embryo-specific expression of soybean oleosin altered oil body morphogenesis and increased lipid content in transgenic rice seeds. Theor Appl Genet 126:2289–2297

Maduka N, Ire FS (2018) Tigernut plant and useful application of tigernut tubers (*Cyperus esculentus*) - A Review. Cur J Applied Sci Technol 29:1–23

Makareviciene V, Gumbytea M, Yunik A, Kalenska S, Kalenskii V, Rachmetov D, Sendzikiene E (2013) Opportunities for the use of chufa sedge in biodiesel production. Ind Crop Prod 50:633–637

Mortazavi A, Williams BA, McCue K, Schaeffer L, Wold B (2008) Mapping and quantifying mammalian transcriptomes by RNA-seq. Nat Methods 5:621–628

Niemeyer PW, Irisarri I, Scholz P, Schmitt K, Valerius O, Braus GH, Herrfurth C, Feussner I, Sharma S, Carlsson AS, de Vries J, Hofvander P, Ischebeck T (2022) A seed-like proteome in oil-rich tubers. Plant J 112:518–534

Ning Y, Li Y, Dong SB, Yang HG, Li CY, Xiong B, Yang J, Hu YK, Mu XY, Xia XF (2023) The chromosome-scale genome of *Kobresia myosuroides* sheds light on karyotype evolution and recent diversification of a dominant herb group on the Qinghai-Tibet Plateau. DNA Res 30:049

Ojha R, Kaur S, Sinha K, Chawla K, Kaur S, Jadhav H, Kaur M, Bhunia RK (2021) Characterization of *oleosin* genes from forage sorghum in *Arabidopsis* and yeast reveals their role in storage lipid stability. Planta 254:97

Qiao X, Li Q, Yin H, Qi K, Li L, Wang R, Zhang S, Paterson AH (2019) Gene duplication and evolution in recurring polyploidization-diploidization cycles in plants. Genome Biol 20:38

Qiao XY, Zheng YJ, Yang JH, Zeng CY, Zou Z (2022a) Gene cloning, subcellular localization and multimerization analysis of *HbPIP1;1* from *Hevea brasiliensis*. Chin J Trop Crops 43:2405–2412

Qiao Z, Kong Q, Tee WT, Lim ARQ, Teo MX, Olieric V, Low PM, Yang Y, Qian G, Ma W, Gao YG (2022b) Molecular basis of the key regulator WRINKLED1 in plant oil biosynthesis. Sci Adv 8:eabq1211

Schein M, Yang Z, Mitchell-Olds T, Schmid KJ (2004) Rapid evolution of a pollen-specific oleosin-like gene family from *Arabidopsis thaliana* and closely related species. Mol Biol Evol 21:659–669

Shimada TL, Shimada T, Takahashi H, Fukao Y, Hara-Nishimura I (2008) A novel role for oleosins in freezing tolerance of oilseeds in *Arabidopsis thaliana*. Plant J 55:798–809

Siloto RMP, Findlay K, Lopez VA, Yeung EC, Nykifork CL, Moloney MM (2006) The accumulation of oleosins determines the size of seed oil bodies in *Arabidopsis*. Plant Cell 18:1961–1974

Singh R, Ong-Abdullah M, Low ET, Manaf MA, Rosli R, Nookiah R, Ooi LC, Ooi SE, Chan KL, Halim MA, Azizi N, Nagappan J, Bacher B, Lakey N, Smith SW, He D, Hogan M, Budiman MA, Lee EK, DeSalle R, Kudrna D, Goicoechea JL, Wing RA, Wilson RK, Fulton RS, Ordway JM, Martienssen RA, Sambanthamurthi R (2013) Oil palm genome sequence reveals divergence of interfertile species in Old and New worlds. Nature 500:335–339

Stoller EW, Sweet RD (1987) Biology and life cycle of purple and yellow nutsedges (*Cyperus rotundus* and *C. esculentus*). Weed Technol 1:66–73

Stoller EW, Weber EJ (1975) Differential cold tolerance, starch, sugar, protein, and lipid of yellow and purple nutsedge tubers. Plant Physiol 55:859–863

Tamura K, Stecher G, Peterson D, Filipski A, Kumar S (2013) MEGA6: molecular evolutionary genetics analysis version 6.0. Mol Biol Evol 30:2725–2729

Turesson H, Marttila S, Gustavsson KE, Hofvander P, Olsson ME, Bülow L, Stymne S, Carlsson AS (2010) Characterization of oil and starch accumulation in tubers of *Cyperus esculentus* var. *sativus* (Cyperaceae): a novel model system to study oil reserves in nonseed tissues. Am J Bot 97:1884–1893

Tzen JT, Lai YK, Chan KL, Huang AH (1990) Oleosin isoforms of high and low molecular weights are present in the oil bodies of diverse seed species. Plant Physiol 94:1282–1289

Wang Y, Tang H, Debarry JD, Tan X, Li J, Wang X, Lee TH, Jin H, Marler B, Guo H, Kissinger JC, Paterson AH (2012) MCScanX: A toolkit for detection and evolutionary analysis of gene synteny and collinearity. Nucleic Acids Res 40:e49

Wang C, Chen L, Cai ZC, Chen C, Liu Z, Liu X, Zou L, Chen J, Tan M, Wei L, Mei Y (2020) Comparative proteomic analysis reveals the molecular mechanisms underlying the accumulation difference of bioactive constituents in *Glycyrrhiza uralensis* fisch under salt stress. J Agric Food Chem 68:1480–1493

Wang L, Jing M, Ahmad N, Wang Y, Wang Y, Li J, Li X, Liu W, Wang N, Wang F, Dong Y, Li H (2021) Tracing key molecular regulators of lipid biosynthesis in tuber development of *Cyperus esculentus* using transcriptomics and lipidomics profiling. Genes (basel) 12:1492

Xiao YH, Zou Z, Zhao YG, Guo AP, Zhang L (2022) Molecular cloning and characterization of an acetolactate synthase gene (*CeALS*) from tigernut (*Cyperus esculentus* L.). Biotech Bull 38:184–192

Xu C, Shanklin J (2016) Triacylglycerol metabolism, function, and accumulation in plant vegetative tissues. Annu Rev Plant Biol 67:179–206

Xu S, Zou Z, Xiao YH, Zhang L, Kong H, Guo JY, Guo AP (2022) Cloning and functional characterization of *CeWRI1*, a gene

involved in oil accumulation from tigernut (*Cyperus esculentus* L.) tubers. Chin J Trop Crop 43:923–929
Yan P, Tuo D, Shen W, Deng H, Zhou P, Gao X (2023) A Nimble Cloning-compatible vector system for high-throughput gene functional analysis in plants. Plant Commun 4:100471
Yee S, Rolland V, Reynolds KB, Shrestha P, Ma L, Singh SP, Vanhercke T, Petrie JR, El Tahchy A (2021) *Sesamum indicum* oleosin L improves oil packaging in *Nicotiana benthamiana* leaves. Plant Direct 5:e343
Yuan Y, Cao X, Zhang H, Liu C, Zhang Y, Song XL, Gai S (2021) Genome-wide identification and analysis of oleosin gene family in four cotton species and its involvement in oil accumulation and germination. BMC Plant Biol 21:569
Zhang HY, Hanna MA, Ali Y, Nan L (1996) Yellow nut-sedge (*Cyperus esculentus* L.) tuber oil as a fuel. Ind Crop Prod 5:177–181
Zhang D, Zhang H, Hu Z, Chu S, Yu K, Lv L, Yang Y, Zhang X, Chen X, Kan G, Tang Y, An YC, Yu D (2019) Artificial selection on *GmOLEO1* contributes to the increase in seed oil during soybean domestication. PLoS Genet 15:e1008267
Zhao YG, Wei WL (2011) Genetic diversity analysis of tigernut (*Cyperus esculentus*) using SRAP markers. Chin J Oil Crop Sci 33:351–355
Zhao X, Yi L, Ren Y, Li J, Ren W, Hou Z, Su S, Wang J, Zhang Y, Dong Q, Yang X, Cheng Y, Lu Z (2023) Chromosome-scale genome assembly of the yellow nutsedge (*Cyperus esculentus*). Genome Biol Evol 15:evad027
Zou Z, Yang JH, Zhang XC (2019) Insights into genes encoding respiratory burst oxidase homologs (RBOHs) in rubber tree (*Hevea brasiliensis* Muell. Arg.). Ind Crop Prod 128:126–139
Zou Z, Zhao YG, Zhang L, Kong H, Guo YL, Guo AP (2021) Single-molecule real-time (SMRT)-based full-length transcriptome analysis of tigernut (*Cyperus esculentus* L.). Chin J Oil Crop Sci 43:229–235
Zou Z, Zhao Y, Zhang L (2022a) Genomic insights into lineage-specific evolution of the *oleosin* family in Euphorbiaceae. BMC Genom 23:178
Zou Z, Zhao YG, Zhang L, Xiao YH, Guo AP (2022b) Analysis of *Cyperus esculentus SMP* family genes reveals lineage-specific evolution and seed desiccation-like transcript accumulation during tuber maturation. Ind Crop Prod 187:115382
Zou Z, Xiao YH, Zhang L, Zhao YG (2023a) Cloning and characterization of *CeEPSPS*, a gene encoding 5-enolpyruvylshikimate-3-phosphate synthase from tigernut (*Cyperus esculentus* L.). Chin J Trop Crop 44:26–34
Zou Z, Xiao YH, Zhang L, Zhao YG (2023b) Analysis of *Lhc* family genes reveals development regulation and diurnal fluctuation expression patterns in *Cyperus esculentus*, a Cyperaceae plant. Planta 257:59
Zou Z, Gong J, An F, Xie G, Wang J, Mo Y, Yang L (2015) Genome-wide identification of rubber tree (*Hevea brasiliensis* Muell. Arg) aquaporin genes and their response to ethephon stimulation in the laticifer, a rubber-producing tissue. BMC Genom 16:1001

Authors and Affiliations

Zhi Zou[1] · Yujiao Zheng[1] · Zhongtian Zhang[1] · Yanhua Xiao[1] · Zhengnan Xie[1] · Lili Chang[1] · Li Zhang[1,2] · Yongguo Zhao[1,3]

✉ Zhi Zou
zouzhi2008@126.com

✉ Li Zhang
zhangli0624@mail.scuec.edu.cn

✉ Yongguo Zhao
zhaoyongguo@gdupt.edu.cn

Yujiao Zheng
zhengyujiaosusie@163.com

Zhongtian Zhang
2424231805@qq.com

Yanhua Xiao
xiao20210924@126.com

Zhengnan Xie
xiezhengnan@itbb.org.cn

Lili Chang
changlili@itbb.org.cn

[1] Hainan Key Laboratory for Biosafety Monitoring and Molecular Breeding in Off-Season Reproduction Regions, Institute of Tropical Biosciences and Biotechnology/Sanya Research Institute of Chinese Academy of Tropical Agricultural Sciences, Haikou 571101, Hainan, People's Republic of China

[2] Hubei Provincial Key Laboratory for Protection and Application of Special Plants in Wuling Area of China, College of Life Science, South-Central Minzu University, Wuhan 430074, Hubei, People's Republic of China

[3] Guangdong University of Petrochemical Technology, Maoming 525000, Guangdong, People's Republic of China